Water Science & Technology

IWA PUBLISHING

Water Science & Technology Vol 87 No 8, 1853 doi: 10.2166/wst.2023.108

Application of soft computing techniques to estimate the scouring depth formed by crossing jets

Reza Mirzaee[a], Mirali Mohammadi [b,*], Sayed-Farhad Mousavi[a], Mohammad Bagherzadeh[b] and Khosrow Hosseini[a]

[a] Department of Water Engineering and Hydraulic Structures, Faculty of Civil Engineering, Semnan University, Semnan, Iran
[b] Department of Civil Engineering, Faculty Engineering, Urmia University, P O Box 165, Urmia 57561-51818, Iran
*Corresponding author. E-mail: m.mohammadi@urmia.ac.ir

MM, 0000-0001-7194-9393

ABSTRACT

The scouring depth caused by the water jet outputs from a dam is one of the crucial parameters for design purposes. Due to the importance of the subject, several laboratory studies have been conducted to understand this subject. Nevertheless, using soft computing techniques is a new attitude for modeling and predicting the natural process parameters. Herein, the types of soft computing techniques for estimating the scouring depth of a plunge pool caused by the symmetrical crossing jets have been explored. The parameters involved in the scouring phenomenon are densimetric Froude number, tailwater depth, vertical jet angle, horizontal crossing angles, and the distance between the crossing points of two jets and the water level. The prediction results show that the Multi-Layer Perceptron (MLP) model gives the best performance among the other models tested here. The Pearson correlation coefficient, root mean square error, and normalized root mean square error for the MLP model were 0.9527, 0.9039, and 19.36% for the test phase, respectively. Furthermore, based on the sensitivity analysis, the parameters, for instance, tailwater depth and vertical jet angle have the highest and lowest effects for predicting the scouring depth of a plunge pool, respectively.

Key words: crossing jet, MLP, plunge pool, scouring, tailwater

HIGHLIGHTS

- Predicting the scour depth of a plunge pool.
- Using different methods of artificial intelligence like Multi-Layer Perceptron (MLP) model, Radial Basis Function (RBF) network, Random Forest Algorithm (RFA), and Multivariate Adaptive Regression Splines (MARS) model.
- Performing sensitivity analysis based on the parameters of the present study.

NOMENCLATURE AND ABBREVIATIONS

α_c	horizontal crossing angles (–)
d_{90}	characteristic diameter of the sediments (m)
D_{eq}	equivalent diameter of jets (m)
g	gravity acceleration (m/s^2)
h_0	tailwater depth (m)
H_{sm}	dimensionless maximum scour depth (–)
ρ	water density (kg/m^3)
S	distance between the crossing point of two jets and water level (m)
T_w	dimensionless tailwater depth (–)
α_c	horizontal crossing angles (–)
D	diameter of the crossing jets (m)
Fr_{d90}	densimetric Froude number (–)
g^*	reduced gravity acceleration (m/s^2)
h_s	maximum scouring depth (m)
δ	dimensionless distance between the crossing point of the two jets and water level (–)

ρ water density (kg/m^3)
SCT Soft Computing Technique
V jet speed in equivalent diameter (m)

1. INTRODUCTION

A plunge pool is one of the most widely used energy dissipation methods in large dams. In those structures, falling jets by impacting with the downstream bed of the dam create a scouring hole which, if the depth of this scour hole is large, can jeopardize the stability of dam and appurtenant structures. Plunge pools are usually used when the tailwater depth is unknown, the materials and bedrock are suitable, and the scour created does not endanger the adjacent structures (Bollaert 2002). For a plunge pool scouring, Canepa & Hager (2003) reported that in the three-phase flow (water, sediment, and air), the scour depth decreases with increasing jet air content. In another study, Pagliara & Palermo (2008) reported that by increasing the angle of jet nozzle, the shape of the scour hole becomes circular, and by decreasing it, the shape of this cavity becomes elliptical.

Pagliara *et al.* (2011a) investigated the plunge pool scouring under symmetrical crossing jets with a fixed vertical angle of 45°. Their results revealed that at low tailwater depth, crossing jets produce a deeper scour compared to single jets. Also, they showed that the distance between the crossing point of the two jets and the water level is an important parameter in estimating the scour depth. The scouring by two vertical crossing jets was studied by Pagliara *et al.* (2012). They presented equations to estimate the dimensions of the scour hole based on the investigated parameters. Pagliara & Palermo (2017) showed that vertical crossing jets caused a longer scour length and a shorter scour depth compared to symmetrical crossing jets and single jets. Shakya *et al.* (2021), by examining the vertical submerged jet scour on a cohesive and non-cohesive sediment bed, showed that the radius of scour hole created in the cohesive sediments was different from non-cohesive sediments.

In the last two decades, researchers have become increasingly interested in using soft computing techniques (SCT) to predict and simulate the behavior of water engineering systems. Some examples of these methods include artificial neural networks (ANN), gene expression programming (GEP), generalized regression of artificial neural networks (GRANN), adaptive neuro-fuzzy inference system (ANFIS), and support vector machine (SVM). By using Ansys Fluent software, Xue *et al.* (2010) investigated the scouring by a submerged jet under the vertical gate. Their results were in good agreement with the experimental data and the most essential and influential parameter in the scour depth was the densimetric Froude number Akib *et al.* (2014) investigated the scour depth under bridge piers using linear regression and the ANFIS method. Their results revealed that the ANFIS method predicted scour depth with high accuracy and less error than the simple linear regression method. Epely-Chauvin *et al.* (2014) studied the plunge pool under a single jet by using Flow-3D software. They showed that the jet angle is a crucial parameter in achieving stable scour depth conditions. Majedi-Asl *et al.* (2017) investigated the scour depth around the bridge piers. They showed that comprehensive prediction of a dependent parameter by SVM gives the most desirable result when the majority of independent parameters affecting the dependent parameter are involved in the prediction process. Yan *et al.* (2020) investigated the scour of vertical jets on non-cohesive sediments by using the modified Eulerian model. Results showed that a good agreement exists between the numerical and experimental output, and the modified Eulerian model simulated the scour depth accurately and effectively. The bridge-pier scour-depth prediction using GEP, SVM, and nonlinear regression was performed by Majedi-Asl *et al.* (2020). Results showed that SVM has better predictability and exemplary performance in estimating scour depth, compared to the other methods. Daneshfaraz *et al.* (2021a) showed that SVM has a good ability to predict vertical drop equipped with a horizontal screen. Numerical simulation and application of soft computing in estimating the energy loss of vertical drop with a horizontal serrated edge were performed by Bagherzadeh *et al.* (2022). In this study, the effect of serrated edge on the energy loss was studied by using Flow-3D software. Then, the energy loss was estimated by using ANN, SVM, and GEP methods. The results of energy loss prediction using SCT showed that all three models have good accuracy for estimating the energy loss, but the accuracy of the ANN method for the test model was higher than the other two methods. Mohammadnezhad *et al.* (2022) estimated the downstream scour depth of a vertical drop by using the SVM algorithm. They showed that the SVM method has appropriate accuracy and acceptable results in estimating the scour depth. Also, it was found that the densimetric Froude number has a greater effect on estimating the relative scouring depth compared to the tailwater depth. Shakya *et al.* (2022) predicted jet scour using soft calculation methods of ANN and multiple nonlinear regression (MNLR). Their study showed that the accuracy of the ANN method is higher than the MNLR method for estimating scour depth due to a jet.

To determine the performance behaviour of hydraulic structures by using experimental models, the cost of construction as well as spending time on conducting experiments are required. On the other hand, by means of artificial intelligence (AI) techniques, AI reduces the cost of physical modeling and the time to reach the results. Also, in those methods, errors such as measurement errors occur during the test elimination. To design a plunge pool as an energy dissipator, the most critical issue is to estimate the initial dimensions of the scouring hole. Since SCT has great ability and accuracy in predicting hydraulic issues and especially scour depth, in the present study, Multi-Layer Perceptron (MLP) method, Radial Basis Function (RBF) network, Random Forest Algorithm (RFA), and Multivariate Adaptive Regression Splines (MARS) model were used to estimate the scour depth caused by the discharge of symmetrical crossing jets into a plunge pool, and the numerical results were compared with some experimental results.

2. METHODOLOGY

2.1. Dimensional analysis

According to Figure 1 and considering the hydraulic parameters of symmetrical crossing jets and sediment characteristics, the resulting scour can be expressed as Equation (1):

$$h_s = f_1(D_{eq}, V, \alpha_c, \alpha_v, S, h_0, g^*, d_{90}) \tag{1}$$

where h_s, D_{eq}, V, α_c, α_v, S, g^*, and d_{90} are the maximum scour depth, equivalent diameter, jet speed in equivalent diameter, horizontal crossing angles, vertical jet angle, distance between the crossing point of two jets and water level, tailwater depth, reduced gravity acceleration, and characteristic diameter of the sediments (sediment particle diameter of which 90% by weight of the particles are smaller, d_{90}), respectively. Note that in the above equation, reduced gravity acceleration and equivalent diameter are equal to: $g^* = [(\rho_s - \rho)/\rho]g$ and $D_{eq} = (2D^2)^{0.5}$, where, ρ_s, ρ, g, and D are sediment density, water density, acceleration due to gravity, and diameter of the crossing jets, respectively. Using the Pi–Buckingham theorem and after a simplification, Equation (1) is expressed as:

$$\frac{h_s}{D_{eq}} = H_{sm} = f_2\left(Fr_{d90} = \frac{V}{\sqrt{g^* d_{90}}}, \alpha_c, \alpha_v, \delta = \frac{S}{D_{eq}}, T_w = \frac{h_0}{D_{eq}}\right) \tag{2}$$

In Equation (2), Fr_{d90} denotes a densimetric Froude number, δ denotes a dimensionless distance between the crossing point of the two jets and the water level, and T_w denotes dimensionless tailwater depth. The range of independent dimensionless parameters is presented in Table 1.

2.2. Experimental characteristics

Experimental data of Pagliara *et al.* (2011b) were used to achieve the objectives of present study. They performed their experiments in a laboratory flume with length, width, and height of 6, 0.8, and 0.9 m, respectively. Two pipes with a diameter of

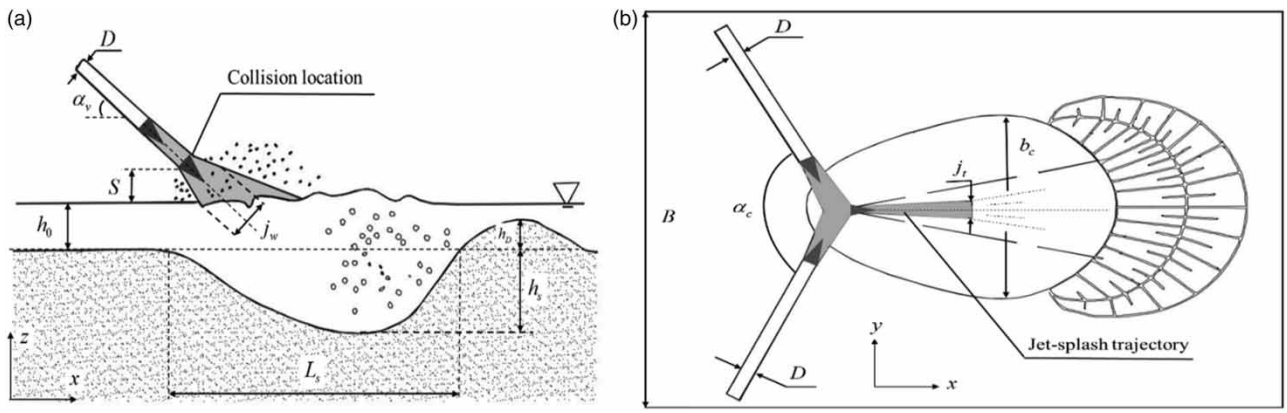

Figure 1 | Schematic of an experimental model: (a) side view and (b) top view (Pagliara *et al.* 2011b).

Table 1 | The range of dimensionless independent parameters (Pagliara *et al.* 2011b)

Parameter	α_c		α_v		Fr_{d90}		T_w		δ	
Range	Min	Max	Min	Max	Min	Max	Min	Max	Min	Max
	30	120	45	85	6.89	14.87	0.7	7.1	0	7

$D = 0.022$ cm were used to make the jet nozzle, and equal discharge flows by two jet nozzles. An ASA-MAG electromagnetic flowmeter with a measurement accuracy of 0.5% was used to measure the discharge rate. Sediment particles with a diameter of $d_{90} = 10.26$ mm and a granulometry of 1.17 (uniform bed) were considered. To create the tailwater depth, a gate in the downstream of flume was used. Pagliara *et al.* (2011b) presented the following analytical equation based on experimental data to estimate the scour depth of symmetrical crossing jets:

$$H_{sm} = a_1 + a_2 T_w + a_3 Fr_{d90} + a_4 \delta + a_5 \alpha_v + a_6 T_w Fr_{d90} + a_7 T_w \delta + a_8 Fr_{d90} \delta + a_9 T_w \alpha_v + a_{10} Fr_{d90} \alpha_v + a_{11} \delta \alpha_v \quad (3)$$

The coefficients used in Equation (3) for different horizontal crossing angles are denoted in Table 2.

2.3. Artificial Neural Networks

ANNs are partly modeled based on the human brain. ANNs can analyze new problems based on previous and pre-learned information. In general, neural networks consist of three layers: input, hidden, and output. The function of the input layer is to introduce the parameters to the network; the output layer is the location of output parameters of the network, and the hidden layer is a layer between the input and output layer that plays the role of information processing (Govindaraju 2000). In general, neural networks are divided into two categories of static and dynamic networks (Kia 2011). For more information, see research provided by Kia (2011).

2.3.1. MLP network

The MLP model is one of the most widely used static networks, which is often used in water science issues. The error replication algorithm and a learning method with an observer were used to train this network. In this model, the number of hidden layers and the number of neurons in each hidden layer are usually determined by using trial and error. A neural network without an activator function is just a linear regression model. Therefore, activation functions solve complex problems in neural networks (Ghorbani *et al.* 2013). In the present research, the quasi-Newton method (Broyden–Fletcher–Goldfarb–Shanno algorithm) was used to train the MLP neural network; the exponential, logistic, and hyperbolic tangent (*Tanh*) functions were used for activation functions of the hidden layer; and the *Tanh* function was used to construct the output layer. To

Table 2 | Coefficients of Equation (3)

	α_c		
Coefficient	30°	75°	120°
a_1	4.938721	5.223549	1.717833
a_2	−0.336533	−0.945931	−0.661428
a_3	0.157614	0.382553	0.486517
a_4	0.245859	−0.506431	−0.180330
a_5	−0.093217	−0.071007	−0.017984
a_6	−0.002492	−0.012897	−0.006818
a_7	−0.099869	−0.086593	−0.074767
a_8	0.002565	−0.009843	−0.006365
a_9	0.008269	0.010977	0.005013
a_{10}	0.003650	0.000086	−0.002834
a_{11}	0.001518	0.006988	0.001927

find the optimal model, the number of neurons in the hidden layer was determined by trial and error (from 3 to a maximum of 11 neurons).

2.3.2. Radial Basis Function

RBF is another type of neural network that offers a different approach to popular neural networks such as MLP with a similar structure. The RBF network solves many different problems, especially classification, patterning, and time series analysis (Haykin 1998). It requires more neurons than standard backpropagation feed–forward neural networks. However, most of those networks can be trained in less time than required for feed–forward networks. In this method, a Gaussian function was used for hidden layer activation functions, and a linear activation function was used to construct the output layer. To get a correct model, the number of neurons in the hidden layers was started from 15 to a maximum of 30 neurons by trial and error. Figure 2 shows the structure of an ANN used in present study.

2.4. Random Forest Algorithm

The performance of RFA is that first, by replacing and constantly changing the practical and goal-related factors, the large number of decision trees is created. Combining those individual trees then increases the accuracy of the predictions (Breiman 2001). Contrary to most machine learning methods, the RFA requires only two parameters to produce a prediction model (Rodriguez-Galiano *et al.* 2015). Number of trees (K) and x-factor that are used in each node to grow regression trees are considered the RFA input variables (Pourghasemi & Rahmati 2018). The RFA includes two powerful ideas, including random selection features and bagging in machine learning algorithms (Breiman 2001; Wu *et al.* 2014). For more information, see research by Breiman (2001). The number of trees in the present study is considered to be 100. A simple outline of the performance of RFA is shown in Figure 3.

2.5. MARS model

The MARS model was first introduced by Friedman (1991). This model is a non-parametric regression method and was presented as a flexible algorithm for organizing the relationship between input parameters and the target variable (Zhang & Goh 2016). The MARS classifies some inputs in the training course using the divide-and-conquer strategy and forms a stepwise regression relationship for each section (Rezaie-Balf *et al.* 2017). Equation (4) gives the value of the Y variable with input x calculated as:

$$Y = \sum_{i=1}^{n} \beta_i B F_i(x) \tag{4}$$

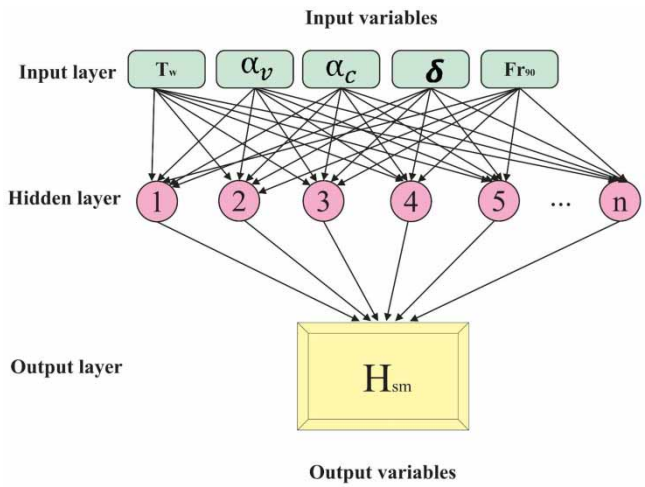

Figure 2 | The ANN structure used for scour depth prediction.

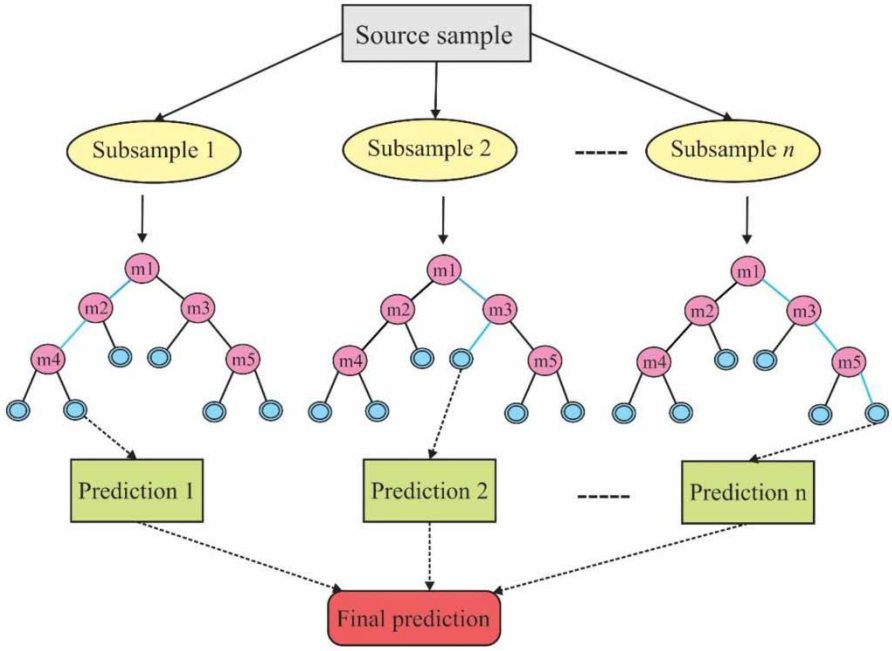

Figure 3 | A schematic flowchart of RFA (Dasineh *et al.* 2021).

In this equation, BF_i, β_i, and n are the basic functions, the weight of the basic function, and the number of the basic functions, respectively. Also, the value of basic functions is calculated from Equations (5) and (6):

$$BF_i = \max(0,\ x - c_i) \tag{5}$$

$$BF_i = \max(0,\ c_i - x) \tag{6}$$

Herein, c_i represents the base node or knot. For more information, see research by Friedman (1991). The MARS model structure is presented in Figure 4. In the implementation settings of the present research model, the maximum number of basic functions is 21, the degree of interaction is 1, the penalty is 2, and the threshold is 0.0005.

2.6. Evaluation criteria

Statistica10 software is used to run all the present study models. The Pearson Correlation Coefficient (*PCC*), Root Mean Square Error (*RMSE*), and Normalized Root Mean Square Error (*NRMSE*) are used to evaluate the accuracy of the models and select the most appropriate forecasting method in the present study (Equations (7)–(9)). In these equations, $H_{sm\ exp}$, $\overline{H}_{sm\ exp}$, $H_{sm\ pre}$, $\overline{H}_{sm\ pre}$, M, and n represent values of the experimental data, mean of the experimental data, values of the data predicted by models, average of the predicted data, average experimental data, and total number of data, respectively (Daneshfaraz *et al.* 2021b, 2021c).

$$PCC = \left(\frac{\sum_{i=1}^{n} (H_{sm\ exp} - \bar{H}_{sm\ exp})(H_{sm\ pre} - \bar{H}_{sm\ pre})}{\sqrt{\sum_{i=1}^{n} (H_{sm\ exp} - \bar{H}_{sm\ exp})^2 \sum_{i=1}^{n} (H_{sm\ pre} - \bar{H}_{sm\ pre})^2}} \right) \tag{7}$$

$$RMSE = \sqrt{\frac{1}{n} \sum_{1}^{n} (H_{sm\ exp} - H_{sm\ pre})^2} \tag{8}$$

$$NRMSE\ (\%) = \frac{RMSE}{M} \times 100 \tag{9}$$

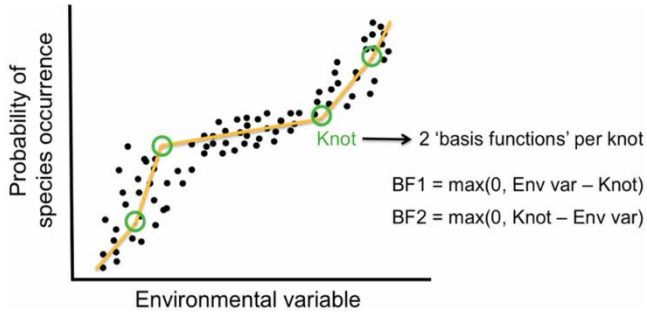

Figure 4 | The sample knots in the MARS model (example knots in MARS).

The *PCC* value varies from −1 to +1, and values close to +1 represent the best model. This criterion indicates the degree of correlation between experimental and predicted values. The *RMSE* criterion ranges from zero to infinity, and values close to zero indicate better model performance; this criterion reports the amount of typical error size. The *NRMSE* criterion for comparing models is classified as follows (Mihoub *et al.* 2016):

Excellent: if $NRMSE < 10\%$.
Good: if $10\% < NRMSE < 20\%$.
Fair: if $20\% < NRMSE < 30\%$.
Poor: if $NRMSE > 30\%$.

3. RESULTS AND DISCUSSION

In the present study, the MLP model, RBF model, RFA, and MARS model were used to estimate the scour depth of a plunge pool under symmetrical crossing jets. Meanwhile, a total of 119 experimental data given by Pagliara *et al.* (2011b) were used, of which 80% of the data (96 data) were used for network training to build a model, and the remaining 20% (23 data) used to test the models. The parameters of Fr_{d90}, T_w, α_v, α_c, and δ were introduced as input to the network. The evaluation criteria of *PCC*, *RMSE*, and *NRMSE* were used to evaluate the accuracy and performance of each model. The training process of the models is repeated several times to minimize errors during the estimation steps. The structure of the models is determined based on trial and error, and its optimal value is considered for each model. Table 3 presents the results of all models implemented for the training and testing stages, and the experimental equation presented by Pagliara *et al.* (2011b).

According to the results of Table 3, it is visible that MLP model evaluation criteria are better than other SCTs, and even Equation (3). Four models (M-1, M-2, M-3, and M-4) via the MLP to predict plunge pool scour depth (five neurons in the input layer (Fr_{d90}, T_w, α_v, α_c, and δ), and one neuron in the output layer (H_{sm})) are considered. Finally, the MLP model (M-1) with 10 neurons in the hidden layer with architecture (5-10-1) and the results of $PCC = 0.9636$, $RMSE = 0.5227$, and $NRMSE = 14.23\%$ for the training phase, and $PCC = 0.9527$, $RMSE = 0.9039$, and $NRMSE = 19.36\%$ for the test phase were recognized as the best model in estimating the scour depth. Results of the models showed that the *PCC* of the training phase was always higher than the test phase. Also, on all models, the error of the training phase was much less than the test phase.

Other prediction models show that they give acceptable results for the scouring issue, which has its complexity. Comparison of the results of experimental Equation (3) with $PCC = 0.9209$, $RMSE = 1.0494$, and $NRMSE = 22.48\%$, and MARS model with $PCC = 0.8996$, $RMSE = 1.1989$, and $NRMSE = 25.68\%$ in the test phase with the results of the MLP model shows that these methods can have good performance in predicting the scour depth with acceptable error. In addition, despite the excellent performance of the RBF and RFA models in most hydraulic investigations, these models could not predict the scour depth of the plunge pool under symmetric crossing jets with high accuracy and low error.

The graphs of scour depth of experimental and predicted models versus the number of data are presented in Figure 5. According to Figure 5, it can be seen that the results of scour depth prediction for the superior model (MLP) in both phases agree with the experimental data. Where scour depth is low, the accuracy of prediction models has increased. In

Table 3 | Performance indicators of ANN-MLP, ANN-RBF, RFA, and MARS models and Equation (3) during the training and testing stages

Model	Structure	Dataset	*PCC*	*RMSE*	*NRMSE (%)*
ANN-MLP					
M-1	**5-10-1**	**Train**	**0.9636**	**0.5227**	**14.23**
		Test	**0.9527**	**0.9039**	**19.36**
M-2	5-3-1	Train	0.9008	0.8597	23.41
		Test	0.8930	1.2497	26.77
M-3	5-6-1	Train	0.9062	0.8285	22.55
		Test	0.8859	1.3559	29.04
M-4	5-7-1	Train	0.9505	0.6098	16.60
		Test	0.9049	1.1586	24.82
ANN-RBF					
R-1	5-22-1	Train	0.8791	0.9506	25.88
		Test	0.8461	1.6808	36.01
R-2	5-20-1	Train	0.8795	0.9269	25.23
		Test	0.8521	1.7544	37.58
R-3	5-30-1	Train	0.8838	0.9156	24.92
		Test	0.8681	1.7494	37.47
R-4	5-23-1	Train	0.8895	0.9035	24.59
		Test	0.8748	1.5526	33.25
RFA	Number of trees = 100, seed for random number generator = 1, minimum n in child node = 5, maximum number of levels = 10, maximum number of nodes = 100	Train	0.8939	0.8829	24.03
		Test	0.8883	1.3024	27.90
MARS	Maximum number of basic functions = 21, degree of interactions = 1, penalty = 2, threshold = 0.0005	Train	0.9119	0.8164	22.23
		Test	0.8996	1.1989	25.68
Equation (3)	———	Train	0.9263	0.7374	20.07
		Test	0.9209	1.0494	22.48

the MLP model, in low values of scour depth, the prediction has promising results with experimental data. In all models, it is observed that the prediction of peak values of scour depth has high errors. Also in the test phase, the superior model reduced the estimation accuracy at the peak values of scour depths. Additionally, in the training phase, the MARS model along with the experimental Equation (3) have recorded a good performance.

To better evaluate the performance of all present studied models, a Violin plot for experimental and predicted data is shown in Figure 6. In this Figure, all results of models are compared with the experimental model in test phase. The similarity of different models to experimental results may provide an excellent understanding to determine the superior model. According to this plot, the MLP model is selected as the superior model of the present study.

3.1. Sensitivity analysis

To determine the effect of any input parameter for estimating the scour depth, it is necessary to perform a sensitivity analysis. For that reason, by removing each one of the parameters from the input list and rerunning the model, its effect on the prediction accuracy was investigated. Figure 7 presents the results of the sensitivity analysis for the present study. According to the results, increasing the T_w reduces the intensity of the jet impact on the bed and causes reduction of the energy and velocity of jets. As a result, increasing the tailwater depth reduces the scour depth of the plunge pool. Therefore, by removing T_w from the input parameters of the superior model, it was observed that the prediction error increased sharply. On the other hand, by increasing the Fr_d, the force due to the jet collision with the bed increases, and the stress due to the jet collision exceeds the critical shear stress of the sediment bed, which leads to an increase

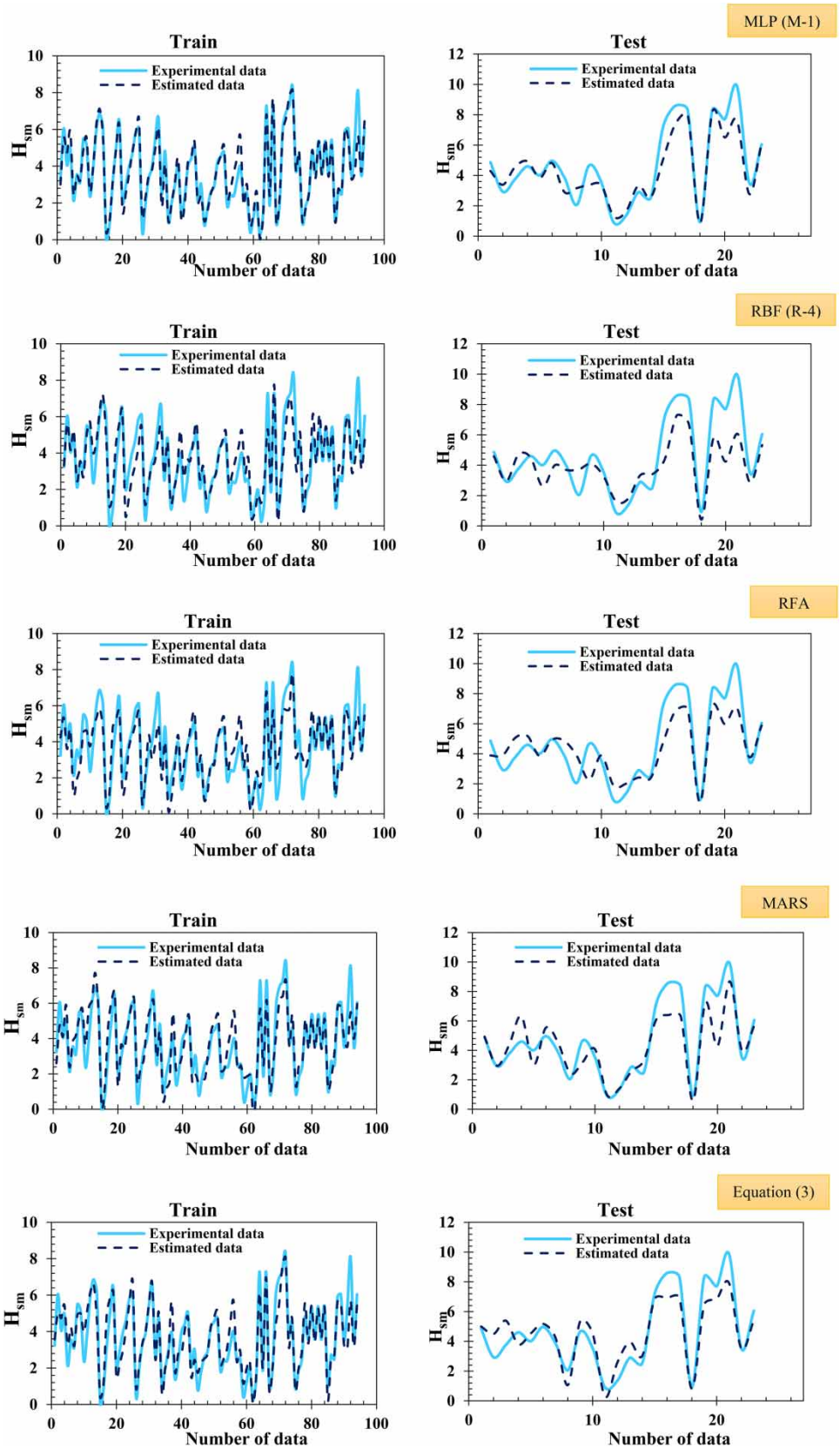

Figure 5 | Experimental and predicted scour depths versus number of data.

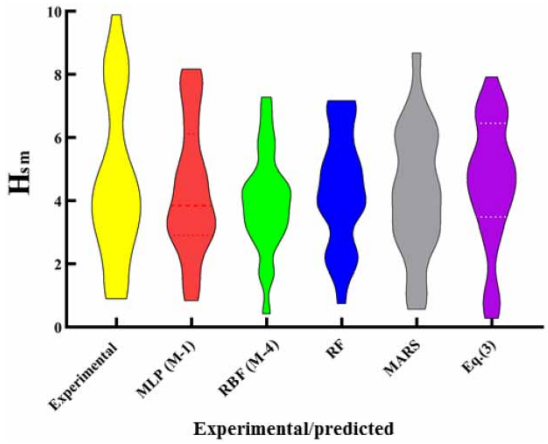

Figure 6 | A Violin plot and comparison of the present study's models with experimental results.

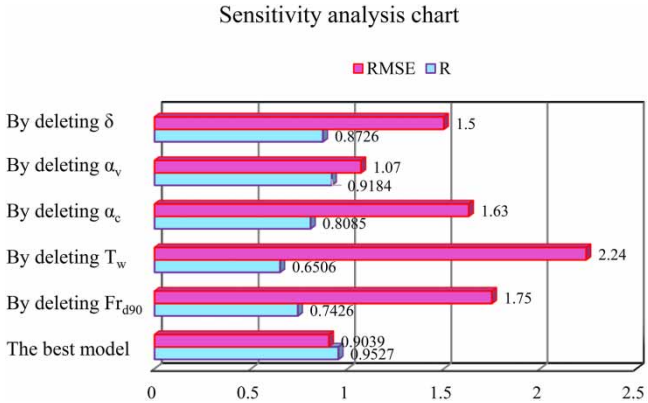

Figure 7 | A sensitivity analysis for the superior model.

in scour depth. In Figure 7, after T_w, the Fr_{d90} is the most effective input parameter. For a low horizontal crossing angle (30°), the collision of two jets has minimal lateral emission, and the performance of crossing jets is similar to a single jet. In contrast, by increasing the horizontal crossing angle, the lateral emission of the jet after collision increases which causes depreciation of the jet's energy, and consequently the scour depth decreases. Consequently, in the MLP model, after T_w and Fr_{d90}, α_c was recognized as an effective one. Moreover, changes in the distance between the crossing point of the two jets and the water level (δ) affect the jet's impact surface with the water level. In other words, with its increase, the surface of the jet's impact with the water level increases and causes the applied force to the bed to decrease. Therefore, an increase in δ leads to a decrease in scour depth. Hence, if δ is used together with T_w and Fr_{d90} in the input list, the prediction error will be reduced. Finally, due to the collision of the jets and their energy dissipation, the effect of the vertical angle of the jets is very small. So, by deleting α_v from the input list, it was observed that the correlation between experimental and predicted data reduced slightly. In other words, the absence of this parameter in the input list of the MLP prediction model did not affect the accuracy of predicting the plunge pool scour depth.

Figure 8 shows the 3D view of the effect of the most influential parameter, T_w, and the least effective parameter, α_v, on the scour depth under symmetrical crossing jets for experimental and predicted data of the superior model. According to Figure 8, it is clear that the presence of T_w has increased the correlation between experimental and predicted data and has the most

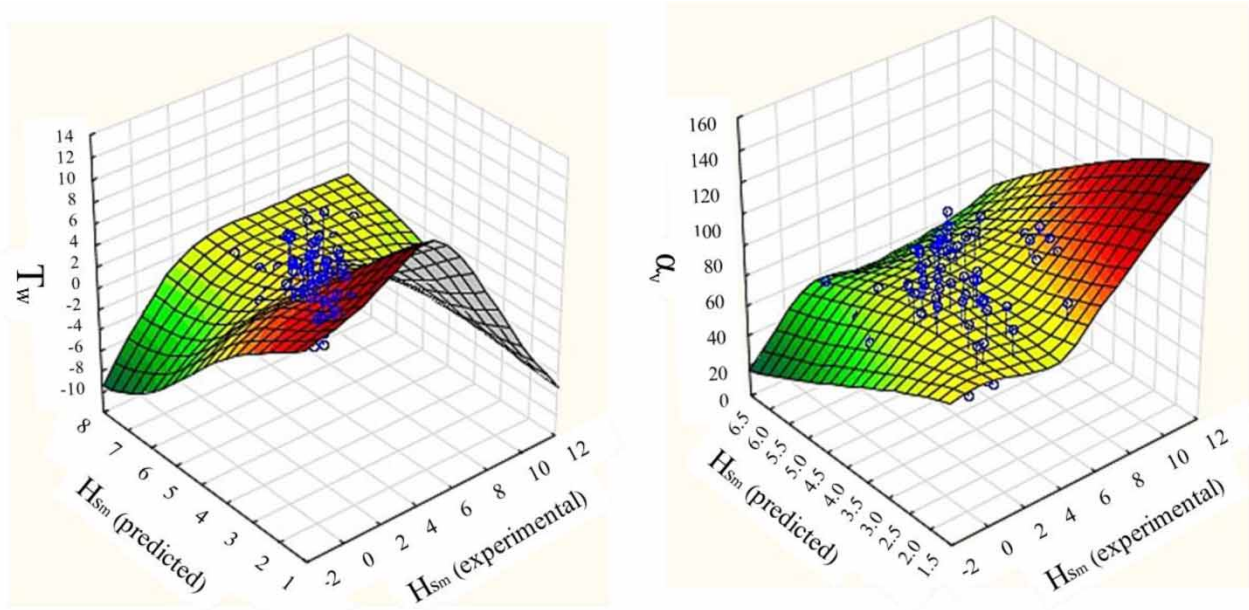

Figure 8 | The influence of T_w and α_v on the scour depth.

excellent effect in estimating the scour depth of the plunge pool. Also, the absence of α_v among the independent input parameters did not have much effect on increasing the prediction accuracy.

4. CONCLUSIONS

The present research aimed to evaluate the performance of MLP, RBF, RFA, and MARS models to predict the scouring depth of a plunge pool under symmetrical crossing jets. For this purpose, 119 series of experimental data were used. Fr_{d90}, T_w, α_v, α_c, and δ were introduced as input parameters to the network, and three evaluation criteria of *PCC*, *RMSE*, and *NRMSE* were used to assess the accuracy of output models and select the best and optimal one. Analysis of the results showed that among all models of the present study, the MLP model (M-1) with 10 neurons in the hidden layer and 5-10-1 architecture, having $PCC = 0.9636$, $RMSE = 0.5227$, and $NRMSE = 14.23\%$ for the training phase and $PCC = 0.9527$, $RMSE = 0.9039$, and $NRMSE = 19.36\%$ for the testing phase, was recognized as the best model for predicting the scour depth. A high correlation between the experimental data and the predicted MLP model, compared to other models and the experimental equation, shows that this method has a high accuracy and acceptable error for estimating the plunge pool scour depth under the symmetrical crossing jets. The results of the present study are satisfactory. Even though estimating the maximum scour depth always presents hydraulic engineers with great challenges; therefore, soft computing methods (e.g. MLP model) can be used to solve the problem. In order to continue the current research, it is recommended that the researchers investigate the effect of the non-uniformity of the sediment particles by applying both the experimental and numerical models prepared. The results, along with other parameters investigated in this research, should be considered as input for the presented models and the best model can be nominated among the others. In addition, the sensitivity analysis reveals that T_w and α_v have the most and the least effect, respectively, for predicting the scouring depth.

ETHICS APPROVAL

The authors are consistent with the ethical requirements.

CONSENT TO PARTICIPATE

The authors all consent to participate in the paper editing.

CONSENT FOR PUBLICATION

The authors all consent to the publication of the paper.

DATA AVAILABILITY STATEMENT

All relevant data are included in the paper or its Supplementary Information.

CONFLICT OF INTEREST

The authors declare there is no conflict.

REFERENCES

Akib, S., Mohammad Hassani, M. & Jahangirzadeh, A. 2014 Application of ANFIS and LR in prediction of scour depth in bridges. *Computers and Fluids* **91**, 77–86.

Bagherzadeh, M., Mousavi, F., Manafpour, M., Mirzaee, R. & Hoseini, K. 2022 Numerical simulation and application of soft computing in estimating vertical drop energy dissipation with horizontal serrated edge. *Water Supply* **22** (4), 4676–4689.

Bollaert, E. 2002 The influence of plunge pool air entrainment on the presence of free air in rock joints. In *Presented at 'Rock Scour due to Falling High-Velocity Jets Conference'*, Lisse, The Netherlands, pp. 137–149. http://infoscience.epfl.ch/record/103498.

Breiman, L. 2001 Random forests. *Machine Learning* **45** (1), 5–32.

Canepa, S. & Hager, W. H. 2003 Effect of jet air content on plunge pool scour. *Journal of Hydraulic Engineering* **129** (5), 358–365.

Daneshfaraz, R., Bagherzadeh, M., Esmaeeli, R., Norouzi, R. & Abraham, J. 2021a Study of the performance of support vector machine for predicting vertical drop hydraulic parameters in the presence of dual horizontal screens. *Water Supply* **21** (1), 217–231.

Daneshfaraz, R., Majedi Asl, M., Mirzaee, R. & Tayfur, G. 2021b Hydraulic jump in a rough sudden symmetric expansion channel. *AUT Journal of Civil Engineering* **5** (2), 4–4. doi:10.22060/ajce.2020.18227.5667.

Daneshfaraz, R., Bagherzadeh, M., Ghaderi, A., Di Francesco, S. & Majedi Asl, M. M. 2021c Experimental investigation of gabion inclined drops as a sustainable solution for hydraulic energy loss. *Ain Shams Engineering Journal* **12** (4), 3451–3459

Dasineh, M., Ghaderi, A., Bagherzadeh, M., Ahmadi, M. & Kuriqi, A. 2021 Prediction of hydraulic jumps on a triangular bed roughness using numerical modeling and soft computing methods. *Mathematics* **9** (23), 3135.

Epely-Chauvin, G., De Cesare, G. & Schwindt, S. 2014 Numerical modelling of plunge pool scour evolution in non-cohesive sediments. *Engineering Applications of Computational Fluid Mechanics* **8** (4), 477–487.

Friedman, J. H. 1991 Multivariate adaptive regression splines. *The Annals of Statistics*, **19**(1), 1–67.

Ghorbani, M. A., Khatibi, R., Hosseini, B. & Bilgili, M. 2013 Relative importance of parameters affecting wind speed prediction using artificial neural networks. *Theoretical and Applied Climatology* **114** (1), 107–114.

Govindaraju, R. S. & ASCE Task Committee on Application of Artificial Neural Networks in Hydrology 2000 Artificial neural networks in hydrology. I: preliminary concepts. *Journal of Hydrologic Engineering* **5** (2), 115–123.

Haykin, S. 1998 Neural networks: a comprehensive foundation. Prentice Hall PTR.

Kia, M. 2011 *Neural Network in MATLAB*. 3rd, Tehran University, Tehran, 229 pp. (In Persian).

Majedi-Asl, M., Valizadeh, S., Ashkan, F. & Hasanzadeh, E. 2017 Modeling scour depth around the inclined single and group piers. *Water and Soil Science* **30** (3), 62–74. (In Persian).

Majedi-Asl, M., Daneshfaraz, R., Fuladipanah, M., Abraham, J. & Bagherzadeh, M. 2020 Simulation of bridge pier scour depth based on geometric characteristics and field data using support vector machine algorithm. *Journal of Applied Research in Water and Wastewater* **7** (2), 137–143. doi:10.22126/arww.2021.5747.1189.

Mihoub, R., Chabour, N. & Guermoui, M. 2016 Modeling soil temperature based on Gaussian process regression in a semi-arid-climate, case study Ghardaia, Algeria. *Geomechanics and Geophysics for Geo-Energy and Geo-Resources* **2** (4), 397–403.

Mohammadnezhad, H., Mohammadi, M. & Bagherzadeh, M. 2022 Estimation of the downstream scour depth of vertical drop using the support vector machine (SVM) algorithm. *Civil Infrastructure Researches*. (in press). doi: 10.22091/cer.2022.8208.1395 (In Persian).

Pagliara, S. & Palermo, M. 2008 Plane plunge pool scour with protection structures. *Journal of Hydro-Environment Research* **2** (3), 182–191.

Pagliara, S., Roy, D. & Palermo, M. 2011a Scour due to crossing jets at fixed vertical angle. *Journal of Irrigation and Drainage Engineering* **137** (1), 49–55.

Pagliara, S., Palermo, M. & Carnacina, I. 2011b Scour process due to symmetric dam spillways crossing jets. *International Journal of River Basin Management* **9** (1), 31–42.

Pagliara, S., Palermo, M. & Roy, D. 2012 Stilling basin erosion due to vertical crossing jets. *Journal of Hydraulic Research* **50** (3), 290–297.

Pagliara, S. & Palermo, M. 2017 Scour process caused by multiple subvertical non-crossing jets. *Water Science and Engineering* **10** (1), 17–24.

Pourghasemi, H. R. & Rahmati, O. 2018 Prediction of the landslide susceptibility: which algorithm, which precision? *Catena* **162**, 177–192.

Rezaie-Balf, M., Zahmatkesh, Z. & Kim, S. 2017 Soft computing techniques for rainfall-runoff simulation: local nonparametric paradigm vs. model classification methods. *Water Resources Management* **31** (12), 3843–3865.

Rodriguez-Galiano, V., Sanchez-Castillo, M., Chica-Olmo, M. & Chica-Rivas, M. J. O. G. R. 2015 Machine learning predictive models for mineral prospectivity: an evaluation of neural networks, random forest, regression trees and support vector machines. *Ore Geology Reviews* **71**, 804–818.

Shakya, R., Sarda, V. K. & Singh, M. 2021 Experimental Study on Scour Due to Submerged Vertical Impinging Circular Jet. In *Transportation, Water and Environmental Geotechnics: Proceedings of Indian Geotechnical Conference* 2020 Volume 4 (pp. 337–345). Singapore.

Shakya, R., Singh, M., Sarda, V. K. & Kumar, N. 2022 Scour depth forecast modeling caused by submerged vertical impinging circular jet: a comparative study between ANN and MNLR. *Sustainable Water Resources Management* **8** (2), 1–10.

Wu, X., Ren, F. & Niu, R. 2014 Landslide susceptibility assessment using object mapping units, decision tree, and support vector machine models in the Three Gorges of China. *Environmental Earth Sciences* **71** (11), 4725–4738.

Xue, W. Y., Huai, W. X. & Qian, Z. D. 2010 Numerical simulation of sediment erosion by submerged plane turbulent jets. *Journal of Hydrodynamics, Ser. B* **22** (5), 593–598.

Yan, X., Mohammadian, A. & Rennie, C. D. 2020 Numerical modeling of local scour due to submerged wall jets using a strict vertex-based, terrain conformal, moving-mesh technique in open FOAM. *International Journal of Sediment Research* **35** (3), 237–248.

Zhang, W. & Goh, A. T. 2016 Multivariate adaptive regression splines and neural network models for prediction of pile drivability. *Geoscience Frontiers* **7** (1), 45–52.

First received 17 October 2022; accepted in revised form 25 March 2023. Available online 11 April 2023